



## 行政院國家科學委員會專題研究計畫成果報告

離子阱質譜儀的正/負化學游離法之溫度、壓力效應研究、串聯質譜靈敏度的測量與冠狀醚的氣相反應

(1) Study of Temperature and Pressure Effect of Negative Chemical Ionization Mass Spectrometry Using Methane and Oxygen as Reagent Gases in an External Source Ion Trap Mass Spectrometer

(2) Examination of the Best Pressure Range for Ion/Molecule Reactions of Anthraquinones in an External Source Ion Trap Mass Spectrometer

(3) Simulation of the Collisional Cooling Effect for Binary and Ternary Buffer Gas Mixtures in a Quadrupole Ion Trap Mass Spectrometer

(4) Determination of Sensitivity of the External Source Ion Trap Tandem Mass Spectrometer Using Dimethyl Ether Chemical Ionization

計畫類別：☒個別型計畫      ☐整合型計畫

計畫編號：NSC89—2113—M—032—024

執行期間：89年8月1日至90年10月31日

計畫主持人：吳慧芬

本成果報告包括以下應繳交之附件：

出席國際學術會議心得報告及發表之論文各一份

執行單位：淡江大學 化學系

中 華 民 國      90 年   10 月   1 日

報告人姓名	吳慧芬	服務機構及職稱	淡江大學化學系教授
會議時間地點	5/27~5/31 美國伊利諾州，芝加哥	本會核定補助文號	NSC-89-2113-M032-024
會議名稱	(中文)第 49 屆美國質譜年會 (英文) 49 <sup>th</sup> ASMS Conference on mass Spectrometry and Allied Topics		
發表論文題目	(中文) 在離子阱質譜儀中，研發選擇性的自身離子/分子反應 (英文) Selective Self - Ion / Molecule Reactions in Ion Trap Mass Spectrometer		
<p>美國質譜學會之年會每年舉辦一次，提供世界各國在質譜科技方面之相關學者、專家研究成果發表與技術相互交流的機會，本研討會長久以來一直為質譜領域最盛大的學術研討會，歷屆舉辦時都吸引許許多多來自世界各地的質譜科技學者與專家的熱烈參與。本次會議為第 49 屆年會，於 2001 年 5 月 27 至 31 日在美國伊利諾州之芝加哥城市舉辦。此次會議的內容除了每天早上 8 點到 10 點的精彩大會的主題演講以外，還有個人的論文發表。論文發表方式分為口頭宣讀與壁報展示兩類。主辦單位這次對於最熱門的生化/蛋白質體方面的主題以及現今質譜科技的幾個重要課題，精心規劃了多項可供聽眾參與的主題，並聘請許多在各個主題及領域內國際知名的學者進行精闢的演講，出席的老師、專家皆仔細聆聽，提出的問題亦獲得熱烈的討論。主辦單位自接受報到、登記註冊、安排會議場地 (Hyatt 旅館)，食宿的安排及其他相關的設備均非常周全及完備，令與會者有賓至如歸之感。配合此次會議，許多家著名的廠商亦參與展出各式新式的質譜儀器，包括最新型的桌上型三段式四極質譜儀及 Bruker 公司所展出的 Q-TOF 電灑質譜儀器，展示會場十分盛大及熱烈，他們所提供的演講也相當精彩。自台灣來參加本研討會的台灣學者共計 7 人，包括中山大學謝建台教授及他的二名博士班學生袁景輝及郭金平，中興大學李茂榮教授，交通大學陳月枝教授、東華大學何彥鵬教授及筆者。每人都有壁報論文的發表。筆者發表的論文題目為：在離子阱質譜儀中，研發選擇性的自身離子/分子反應。本篇論文屬於壁報論文展示，被安排在 5 月 30 日下午。這次能夠獲得國科會在經費上的補助參加本屆質譜國際性學術的研討會，筆者感到相當的高興。視野大大地擴展，對研究方面的興趣大大地提昇，更鼓舞筆者在研究方面的士氣，對於筆者的研究靈感的激發亦有相當大之功效。筆者在此深深地感謝國科會所提供的寶貴機會。期望國科會以後能繼續鼓勵及補助國內有心做研究的學者或專家踴躍參加國際性的研討會，相信對於個人學術研究水準之提昇，及我國整體國際之學術研究地位的提高將有最快速的功效。</p> <p>筆者這次在五天的研討會之中，收穫滿滿的，尤其是在個人研究領域之氣相離子/分子反應方面，今年這方面的研究成果相當豐碩，也讓筆者大開眼界，學到許多東西。但是，由於時差的關係，確實覺得很疲倦，但與學習到的收穫及成果對個人研究方面的增益比較起來，這些小問題都微不足道了。</p> <p>攜回資料名稱及內容： 筆者發表的論文摘要，研討會議程及研討會邀請函，請見附件</p>			

## Selective Self - Ion / Molecule Reactions in Ion Trap Mass Spectrometer

Hui-Fen Wu; Ming-Yi Ho; Chien-Hung Chen

Chemistry Department, Tamkang University, Taipei Hsien, Taiwan

### Introduction:

A new identification method in mass spectrometry based on the Selective Self - Ion / Molecule Reactions (SSIMR) in both external and internal source Ion Trap Mass Spectrometers was demonstrated. Selective self-ion/molecule reaction product ions were produced between the oxygenated and nitrogenated crown ethers and their acyclic analogues. For the oxygenated crown ethers, Self-Ion/Molecule Reactions lead to the formation of the protonated ions, adduct ions of fragments, while the nitrogenated crown ethers produce protonated molecules,  $[M+13]^+$  and  $[M+27]^+$  ions. Glymes produce protonated molecules and fragments with the character of elimination of one molecule of methanol. Glycols produce protonated molecules and fragment ions via elimination of one molecule of water.

### Experimental:

The experiments were performed using both external (Finnigan GCQ) and internal source ion trap mass spectrometers (Varian GC/MS). The ion trap was operated in the mass selective instability mode for detection of ions. No CI reagent gas was used in both instruments. Samples were introduced to the ion trap by Gas Chromatography (GC) or to the ion source region via a temperature controlled direct insertion probe (DIP) to assist the desorption of the samples.

### Results and Discussion:

#### (1) Observation of Selective Self-Ion/Molecule Reactions:

Heterodonor atom effect was observed between the oxygenated and nitrogenated crown ethers from the results of SSIMR. The SSIMR provides two advantages. First, formation of the characteristic peaks due to SSIMR are useful for the identification of unknown compounds in the future applications. Second, no chemical reagent is needed to perform selective ion/molecule reactions. Thus, it is very convenient, easy to use and economic.

#### (2) Experimental method to prove the source and reaction mechanism:

In the absence of reagent gas, SSIMR can take place by reaction of the low-mass fragment ions of crown ethers with the neutral crown ether molecules. In order to determine which ions are protonating the crown ether derivatives by selectively storing each of the fragment ions appeared in the mass spectrum in turn. Each specific fragment ion was isolated by a broadband waveform

to eject all other unwanted ions, and then the isolated fragment ion was allowed to react with the neutral crown ethers present in the trap for a period of 60 ms. After the reaction time, formation of the product ions can prove the source of the SSIMR.

(3) Study of the Concentration Effect:

Constant amount of sample being introduced into both instruments is necessary since the fluctuation of the concentration of the sample may lead to the variation of SSIMR. The sample amount introduced into GCQ via DIP was 30 $\mu$ g. Although the internal source ion trap is intentionally operated favor for the conditions for the occurrence of ion/molecule reactions, the SSIMR obtained in the internal source ion trap seem much weaker than that obtained in the external source ion trap. This is due to the concentration effect. Since only 1  $\mu$ g of samples were introduced into the internal source ion trap by GC. This reveals that the concentration effect plays an important role in SSIMR.



**49th ASMS Conference on Mass Spectrometry and Allied Topics**  
Chicago, Illinois  
May 27-31, 2001

## Program Highlights

<b>Sunday</b>	<p>10:00 am - 8:00 pm 5:00 - 6:30 pm  7:00 - 9:00 pm</p>	<p><b>REGISTRATION</b> <b>TUTORIAL LECTURES</b>  <ul style="list-style-type: none"> <li>• <b>Franz Hillenkamp &amp; Klaus Dreisewerd:</b> <i>"Desorption Lasers in Mass Spectrometry: Choices and Selections"</i></li> <li>• <b>Jennifer Brodbelt:</b> <i>"Quadrupole Ion Traps: Fundamentals and New Applications"</i></li> </ul> <b>WELCOME MIXER</b></p>
<b>Monday</b>	<p>7:30 am 8:00 - 8:45 am 8:45 - 10:15 am 10:15 am - 12:15 pm  12:15 - 1:30 pm 1:30 - 3:00 pm 3:00 - 5:00 pm  5:30 - 7:00 pm 6:30 - midnight</p>	<p><b>WAKE-UP COFFEE</b>  <b>PLENARY LECTURE:</b> Steffan Nilsson, Lund University; <i>"Airborne Cell Analysis"</i>  <b>POSTER SESSIONS AND EXHIBITS</b>  <b>ORAL SESSIONS</b> <ul style="list-style-type: none"> <li>• Proteomics - New Technologies</li> <li>• Ionization Processes</li> <li>• FTICR MS Innovations</li> <li>• LC/MS - High Flow</li> <li>• Environmental Chemistry - General</li> </ul> <b>LUNCH BREAK AND INTEREST GROUP MEETINGS</b>  <b>POSTER SESSIONS AND EXHIBITS</b>  <b>ORAL SESSIONS</b> <ul style="list-style-type: none"> <li>• Ion Activation / Dissociation - Greater than 1 kDa</li> <li>• Reactions of Trapped Ions</li> <li>• Novel Uses of Standard Instruments</li> <li>• Carbohydrate Sequencing</li> <li>• Environmental - Emerging Contaminants</li> </ul> <b>WORKSHOPS</b>  <b>CORPORATE HOSPITALITY SUITES</b></p>
<b>Tuesday</b>	<p>7:30 am 8:00 - 8:45 am 8:45 - 10:15 am 10:15 am - 12:15 pm  12:15 - 1:30 pm 1:30 - 3:00 pm 3:00 - 5:00 pm  5:30 - 7:00 pm 6:30 - midnight</p>	<p><b>WAKE-UP COFFEE</b>  <b>AWARD LECTURE:</b> Recipient of the Award for a Distinguished Contribution in Mass Spectrometry  <b>POSTER SESSION AND EXHIBITS</b>  <b>ORAL SESSIONS</b> <ul style="list-style-type: none"> <li>• Biomacromolecular Complexes</li> <li>• Ion Activation / Dissociation - Small Molecules</li> <li>• Designs for the Future</li> <li>• Glycoconjugates</li> <li>• Drugs - Metabolite Identification</li> </ul> <b>LUNCH BREAK AND INTEREST GROUP MEETINGS</b>  <b>POSTER SESSION AND EXHIBITS</b>  <b>ORAL SESSIONS</b> <ul style="list-style-type: none"> <li>• Proteins - Alternatives to 2D Gels</li> <li>• Immunology</li> <li>• Quadrupole Ion Traps - New Designs</li> <li>• DNA / RNA Sequencing</li> <li>• Drugs - High Throughput</li> </ul> <b>WORKSHOPS</b>  <b>CORPORATE HOSPITALITY SUITES</b></p>

## Program Highlights

<b>Wednesday</b>	7:30 am	<b>WAKE-UP COFFEE</b>
	8:00 – 8:45 am	<b>AWARD LECTURE: Recipient of the Biemann Medal</b>
	8:45 – 10:15 am	<b>POSTER SESSION AND EXHIBITS</b>
	10:15 am – 12:15 pm	<b>ORAL SESSIONS</b> <ul style="list-style-type: none"> <li>• Protein Conformations</li> <li>• Microbes and Parasites</li> <li>• Lipids – Oxidative Stress Markers</li> <li>• Ion Structures and Energetics</li> <li>• Ion Chromatography</li> <li>• Polymer Synthesis</li> </ul>
	12:15 – 1:30 pm	<b>LUNCH BREAK AND INTEREST GROUP MEETINGS</b>
	1:30 – 3:00 pm	<b>POSTER SESSION AND EXHIBITS</b>
	3:00 – 5:00 pm	<b>ORAL SESSIONS</b> <ul style="list-style-type: none"> <li>• Proteins – Interactions with Metals</li> <li>• Diagnosis of Disease</li> <li>• TOF Analyzer Development</li> <li>• LC/MS – Microscale</li> <li>• Charge Permutation / Transfer</li> <li>• Polymer MS/MS</li> </ul>
	5:30 – 6:30 pm	<b>ASMS BUSINESS MEETING</b>
	6:30 - midnight	<b>CORPORATE HOSPITALITY SUITES</b>
<b>Thursday</b>	7:30 am	<b>WAKE-UP COFFEE</b>
	8:00 – 8:45 am	<b>PLENARY LECTURE: John M. Hayes, Woods Hole Oceanographic Institute, "Molecular-Isotopic Studies of Biogeochemical Processes"</b>
	8:45 – 10:15 am	<b>POSTER SESSION AND EXHIBITS</b>
	10:15 am – 12:15 pm	<b>ORAL SESSIONS</b> <ul style="list-style-type: none"> <li>• The Extracellular Matrix</li> <li>• Teaching Mass Spectrometry</li> <li>• Microfabrication / Microfluidics</li> <li>• Imaging / Surface Analysis</li> <li>• Isotope Ratio MS</li> <li>• Hydrocarbons – New Approaches to Old Problems</li> </ul>
	12:15 – 1:30 pm	<b>LUNCH BREAK AND INTEREST GROUP MEETINGS</b>
	1:30 – 3:00 pm	<b>POSTER SESSION AND EXHIBITS</b>
	3:00 – 5:00 pm	<b>ORAL SESSIONS</b> <ul style="list-style-type: none"> <li>• Proteomics – Medical Applications</li> <li>• Protein Folding</li> <li>• Computer Applications</li> <li>• MS vs. Spies and Sports Abuse</li> <li>• Natural Products with Drug Potential</li> <li>• Hydrocarbons – Future Challenges</li> </ul>
	5:30 – 6:30 pm	<b>PLENARY LECTURE: "The Science of Art"</b>
	6:30 – 10:00 pm	<b>CONFERENCE FINALE: The Art Institute of Chicago</b>



**49th ASMS Conference on Mass Spectrometry and Allied Topics**  
 Chicago, Illinois  
 May 27-31, 2001

## JMS Letters

Dear Sir,

### Study of temperature and pressure effects of negative chemical ionization mass spectrometry using methane and oxygen as reagent gases in an external source ion trap mass spectrometer

Negative chemical ionization (NCI) mass spectrometry is an ideal technique for the analysis of compounds containing electrophilic groups owing to its high sensitivity and selectivity.<sup>1–17</sup> It has been applied to the analysis of many compounds in traditional mass spectrometers including the quadrupole<sup>2,3,6,9–12</sup> and magnetic sector<sup>7</sup> types, but not using ion trap mass spectrometry (ITMS) since it was difficult to achieve NCI measurements with the classical ion trap. Therefore, very few reports have discussed the use of ITMS for negative ion analysis.<sup>13,15</sup> The reason is the very low efficiency of negative-ion formation via electron capture when 70 eV electrons are used. However, since 1996, when the first commercial ion trap mass spectrometer with an external ionization source (Finnigan MAT GCQ)<sup>16,17</sup> appeared on the market, negative ions could be detected. The reasons are that the GCQ allows operation at higher pressures at the ion source region (1 mTorr; 1 Torr = 133.3 Pa) and also possesses a modified detector with a conversion dynode ( $\pm 15$  kV). NCI is very sensitive to the effects of reagent gas pressure<sup>9,10,12,14</sup> and ion source temperature<sup>6–9,11,12,14</sup> in traditional mass analyzers. Further, NCI has shown more significant temperature effects than positive chemical ionization (PCI) in quadrupole and sector mass analyzers.<sup>1–5</sup> The source temperature effect on the PCI of dopamine with dimethyl ether (DME) ions has been evaluated with the GCQ.<sup>17</sup> In this study, the effects of reagent pressure and source temperature for NCI measurements were studied for the first time using the GCQ.

All experiments were carried out in an external source ion trap mass spectrometer (Finnigan MAT GCQ). Methane and oxygen were used as the CI reagent gases. The pressure of the CI gas ranged from 0.021 to 0.13 Pa. The instrument was operated in the mass-selective instability mode. The pressure of He was 0.13 Pa. All pressures were measured with an ion gauge mounted on the vacuum chamber. The ion source and transfer line temperatures were 200 and 225 °C, respectively. The ion source region was heated by three cartridge heaters and the source temperature was measured by a platinum probe temperature sensor. The ion injection time was 0.3–25 ms. Sample were introduced to the ion source via a direct insertion probe (DIP). The probe tip was heated to a temperature of 150–370 °C depending on compounds.

When methane or oxygen was used as the reagent gas in the NCI mode in the GCQ, no reagent ions were produced. In fact, they act as a moderator. A large number of thermal electrons were produced, which can be captured by high electron affinity molecules. In the NCI measurements, few fragment ions were observed by the electron capture (EC) mechanism in the GCQ since the captured electrons possess low energy. In order to understand the effects of the source temperature and reagent gas pressure in the GCQ, NCI experiments on 3,4,5,6-tetrachlorophthalimide were performed and the results are given in Table 1 as the ratios of the relative signal intensity of the fragment ion  $[M - HCl]^-$  ( $m/z$  247) to that of the molecular anion  $M^-$  ( $m/z$  285). From Table 1, the signal intensity of the fragment ion

Table 1. Temperature and pressure effects of 3,4,5,6-tetrachlorophthalimide

Temperature (°C)	Relative intensity ratio <sup>a</sup>		
	0.021 Pa	0.084 Pa	0.13 Pa
100	0.29	0.03	0.06
120	0.38	0.05	0.06
140	0.69	0.04	0.06
160	0.90	0.08	0.08
180	1.37	0.07	0.09
200	1.19	0.06	0.10

<sup>a</sup> Relative signal intensity of  $[M - HCl]^-$  ( $m/z$  247) / relative signal intensity of  $M^-$  ( $m/z$  285).

increases as the temperature increases at all pressures. However, as the pressure reaches to 0.13 Pa, the temperature effect becomes less significant. For example, at a source temperature of 100 °C, the above ratio decreases from 0.29 to 0.06 as the reagent pressure increases from 0.021 to 0.13 Pa. However, at a source temperature of 200 °C, the ratio decreases from 1.19 to 0.10. These results indicate that as the reagent pressure reaches 0.13 Pa, the formation of  $M^-$  is favored. The reason is that at higher reagent gas pressure, the thermal electrons can be produced more effectively (with a larger population) in order to stabilize the  $M^-$  ions. Hence fewer fragment ions were obtained. Table 2 shows the source temperature effect on the NCI experiments for 5-fluorouracil. The pressure of methane was maintained at  $5.3 \times 10^{-2}$  Pa. The temperature of the ion source was varied from 100 to 200 °C. There were no significant changes in the relative abundance of any of the ions except for the  $[2M - H]^-$  ions, for which the relative abundance increased from 12 to 32% as the temperature increased from 100 to 200 °C. Since a pressure of  $5.3 \times 10^{-2}$  Pa was sufficient to stabilize the product ions, the variation of temperature did not affect the product ions except for the  $[2M - H]^-$  ions which may due to a higher reaction rate at higher source temperatures.<sup>17</sup>

The NCI spectra obtained with methane and oxygen as reagent gases for several phthalic anhydride derivatives are compared in Table 3. All compounds produce oxygenated ions ( $[M - X + O]^-$ , where  $X = Cl$  or  $Br$ ) in the oxygen spectra but not in the methane spectra, except for 3,4,5,6-tetrafluorophthalic anhydride. The formation mechanism for the  $[M - Cl/Br + O]^-$  ion is due to the nucleophilic reaction of the neutral molecule ( $M$ ) with oxygen ions.

Table 2. Source temperature effect on the relative abundance (%) of ions in NCI spectra of 5-fluorouracil

Product ( $m/z$ )	Temperature (°C)				
	100	125	150	175	200
$2M^-$ (260)	1	1	4	2	2
$[2M - H]^-$ (259)	12	11	13	21	32
$M^-$ (130)	18	5	5	5	5
$[M - H]^-$ (129)	100	100	100	100	100
$[2M - HF]^-$ (240)	4	2	2	3	1
$[(2M - H) - (HF + F)]^-$ (220)	4	4	4	4	2
$[(2M - H) - (HF + F + CO)]^-$ (192)	2	2	2	2	2
$[(2M - H) - (HF + F + CO + HCN)]^-$ (165)	7	7	9	7	6
144 <sup>-</sup>	18	2	1	1	<1
111 <sup>-</sup>	1	2	2	1	<1
$NCO^-$ (42)	5	4	3	3	1

\* Correspondence to: H.-F. Wu, Department of Chemistry, Tamkang University, Tamsui, Taipei Hsien 25137, Taiwan.

Contract/grant sponsor: National Science Council of the Republic of China; Contract/grant number: NSC 89-2113-M-032-024.

Contract/grant sponsor: Tamkang University.

Table 3. ECD results using CH<sub>4</sub> and oxygen as reagent gases

Compound ( <i>m/z</i> )	O <sub>2</sub>		Reagent gas	
			CH <sub>4</sub>	
4,5-Dichlorophthalic anhydride (216)	M <sup>••</sup>	(216, 7%)	M <sup>••</sup>	(216, 100%)
	[M - <sup>35</sup> Cl + O] <sup>-</sup>	(197, 100%)	[M + OH] <sup>-</sup>	(233, 18%)
	[M - <sup>37</sup> Cl + O] <sup>-</sup>	(195, 46%)	[M + OH - <sup>35</sup> Cl] <sup>-</sup>	(198, 4%)
3,4,5,6-Tetrafluorophthalic anhydride (220)	M <sup>••</sup>	(220, 100%)	[M + OH - <sup>37</sup> Cl] <sup>-</sup>	(196, 2%)
	M <sup>••</sup>	(220, 100%)	M <sup>••</sup>	(220, 100%)
3,4,5,6-Tetrachlorophthalic anhydride (286)	M <sup>••</sup>	(286, 100%)	M <sup>••</sup>	(286, 100%)
	[M - <sup>35</sup> Cl + O] <sup>-</sup>	(267, 8%)		
	[M - <sup>37</sup> Cl + O] <sup>-</sup>	(265, 8%)		
	[M - <sup>35</sup> Cl <sup>37</sup> Cl + O] <sup>-</sup>	(230, 2%)		
3,4,5,6-Tetrabromophthalic anhydride (464)	M <sup>••</sup>	(464, 100%)	M <sup>••</sup>	(464, 20%)
	[M - <sup>79</sup> Br + O] <sup>-</sup>	(401, 81%)	[M - <sup>79</sup> Br] <sup>-</sup>	(384, 100%)
	[M - <sup>81</sup> Br + O] <sup>-</sup>	(399, 87%)	[M - <sup>81</sup> Br] <sup>-</sup>	(386, 24%)
	Br <sup>-</sup>	(81, 16%)	Br <sup>-</sup>	(81, 82%)
	Br <sup>-</sup>	(79, 15%)		

### Acknowledgements

We acknowledge support from the National Science Council of the Republic of China (Grant No. NSC 89-2113-M-032-024) and Tamkang University.

Yours,

HUI-FEN WU\*

Department of Chemistry, Tamkang University, Tamsui, Taipei Hsien 25137, Taiwan.

### References

1. Dillard JG. *Chem. Rev.* 1973; **73**: 589.
2. Hunt DF, Stafford GC Jr, Crow FW, Russell JW. *Anal. Chem.* 1976; **48**: 2098.
3. Hunt DF, Crow FW. *Anal. Chem.* 1978; **50**: 1781.
4. Bowie JH. *Mass Spectrom. Rev.* 1984; **3**: 161.
5. Budzikiewicz H. *Mass Spectrom. Rev.* 1986; **5**: 345.
6. Oehme M, Stockl D, Knoppel H. *Anal. Chem.* 1986; **58**: 554.
7. Tannenbaum HP, Roberts JD, Dougherty RC. *Anal. Chem.* 1975; **47**: 49.
8. Hahndorf I, Illenberger E. *Int. J. Mass Spectrom. Ion Processes* 1997; **167/168**: 87.
9. Hilpert LR, Byrd GD, Vogt CR. *Anal. Chem.* 1984; **56**: 1842.
10. Laramée JA, Arbogast BC, Deinzer ML. *Anal. Chem.* 1986; **58**: 2907.
11. Trainor JM, Vouros P. *Anal. Chem.* 1987; **59**: 601.
12. Ramdahl T, Urdal K. *Anal. Chem.* 1982; **54**: 2256.
13. McLuckey SA, Glish GL, Kelley PE. *Anal. Chem.* 1987; **59**: 1670.
14. Oehme M. *Anal. Chem.* 1983; **55**: 2290.
15. Catinella S, Traidi P, Jiang X, Londry FA, Morrison RJS, March RE, Gregoire S, Mathurin J-C, Tabet J-C. *Rapid Commun. Mass Spectrom.* 1995; **9**: 1302.
16. Wu H-F, Lin Y-P. *J. Mass Spectrom.* 1999; **34**: 1283.
17. Wu H-F, Lin Y-P. *Eur. Mass Spectrom.* In press.



## Examination of the Best Pressure Range for Ion/Molecule Reactions of Anthraquinones in an External Source Ion Trap Mass Spectrometer

Hui-Fen WU,<sup>†</sup> Chien-Hung CHEN, and Ming-Yi Ho

Department of Chemistry, Tamkang University, Tamsui, Taipei Hsien, 25137, Taiwan, R. O. C.

This study outlines some observations of the pressure effect for gas phase ion-molecule reactions of anthraquinone derivatives with dimethyl ether in an external source ion trap mass spectrometer. At the reagent pressure of  $7.998 \times 10^{-2}$  Pa, formation of the protonated ions,  $[M + 13]^+$ ,  $[M + 15]^+$ , and  $[M + 45]^+$  ions, of anthraquinones can be observed. However, at the pressure of  $1.066 \times 10^{-2}$  Pa, formation of molecular ions and many fragment ions of the  $M^+$  or  $[M + H]^+$  ions have been observed. Since the pressure effect is notable within a small range of pressures for many compounds, it is important to draw attention to the use of the ion trap with an external source where other factors such as ion source residence time may play a role. This can also provide some information for better and more careful controls of the reagent pressure in order to obtain fair CI spectra in an external source ion trap mass spectrometer.

(Received October 10, 2000; Accepted January 9, 2001)

### Introduction

Dimethyl ether (DME) has been widely used as the positive chemical ionization (PCI) reagent gas in an ion trap mass spectrometer (ITMS).<sup>1-21</sup> Ion/molecular reaction products including  $[M + H]^+$ ,  $[M + 13]^+$ ,  $[M + 15]^+$ ,  $[M + 45]^+$  and  $[M + 47]^+$  ions can be produced in the ITMS depending on the structures of compounds.<sup>1-21</sup> However, all these studies have been undertaken in a traditional internal chemical ionization ion trap mass spectrometer. Since 1996, the Finnigan MAT Company has produced a bench-top external source ion trap mass spectrometer (GCQ). Up to date, very few studies about CIMS of the external source ion trap mass spectrometer have been reported.<sup>22,23</sup> Therefore, we decided to investigate the DME CIMS in GCQ by performing ion-molecule reactions with several anthraquinone compounds. The structures of anthraquinones are shown in Fig. 1.

### Experimental

All experiments have been performed in an external source ion trap mass spectrometer (Finnigan MAT GCQ).<sup>22-24</sup> Several reagent ions including  $m/z$  45 ( $CH_3O=CH_2^+$ ),  $m/z$  47 ( $CH_3OHCH_2^+$ ),  $m/z$  61 ( $(CH_3)_2O^+$ ),  $m/z$  91 ( $(CH_3)_2O^+CH_2OCH_3$ ) and  $m/z$  93 ( $(CH_3)_4O_2H^+$ ), are produced when dimethyl ether is applied as CI reagent gas in the external source ion trap. Only  $m/z$  45 and 47 ions exhibit chemical reactivity, leading to the formation of ion/molecular reaction products including  $[M + H]^+$ ,  $[M + 13]^+$ ,  $[M + 15]^+$ ,  $[M + 45]^+$  and  $[M + 47]^+$  ions.<sup>21</sup> In our experiments, the relative intensity of these reagent ions was also pressure dependent. The relative intensities for  $m/z$  45, 47,

61, 91 and 93 at  $1.066 \times 10^{-2}$  Pa are 100, 82, 13, 1 and 4%, respectively, while the relative intensities for  $m/z$  are 45, 47, 61, 91 and 93 at  $7.998 \times 10^{-2}$  Pa are 62, 28, 100, 16 and 33%, respectively. The pressure of He was 1 mTorr. DME pressure in GCQ can be measured by using a convection gauge, but the pressure we report in this study was measured by an ion gauge in order to measure the pressure precisely. The pressure of DME was controlled at two different levels of  $1.066 \times 10^{-2}$  and  $7.998 \times 10^{-2}$  Pa to examine the pressure effect.

The experimental pressure range is rather small. The reason for this is that the ion gauge was installed on the vacuum chamber, rather than at the source region for GCQ. If the pressure is measured by a convection gauge at the source region, the pressure ranges from 2.666 - 10.664 Pa. The ion source was maintained at constant temperature of 200°C by using three cartridge heaters and the source temperature was measured by the platinum probe temperature sensor.

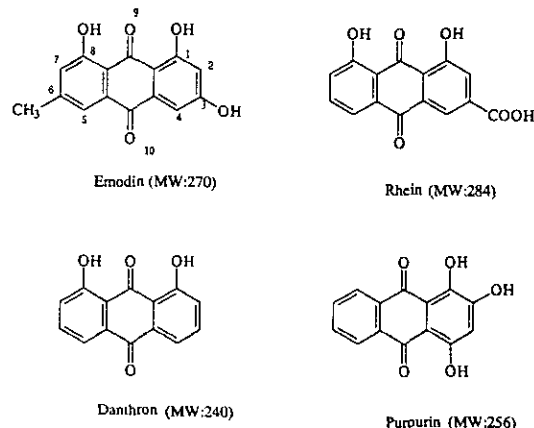


Fig. 1 Structures of anthraquinone derivatives.

<sup>†</sup> To whom correspondence should be addressed.

E-mail: gou@mail.tku.edu.tw

Table 1 Ion-molecule reaction products of anthraquinones and dimethyl ether ions at  $7.988 \times 10^{-2}$  Pa

Compound (Mw)	Product ion ( <i>m/z</i> , relative intensity)
Emodin (270)	[M+47] <sup>+</sup> (317, <1%)
	[M+45] <sup>+</sup> (315, 20%)
	[M+15] <sup>+</sup> (285, 42%)
	[M+13] <sup>+</sup> (283, 30%)
	[M+H] <sup>+</sup> (271, 100%)
	M <sup>+</sup> (270, <1%)
	[M-H] <sup>+</sup> (269, 30%)
Danthron (240)	[M+47] <sup>+</sup> (287, <1%)
	[M+45] <sup>+</sup> (285, 5%)
	[M+15] <sup>+</sup> (255, 5%)
	[M+H] <sup>+</sup> (241, 100%)
	M <sup>+</sup> (240, 30%)
	[M-CO] <sup>+</sup> (212, 8%)
	[M-2CO] <sup>+</sup> (184, 5%)
Rhein (284)	[M-2CO-2x28] <sup>+</sup> (128, 2%)
	[M+47] <sup>+</sup> (331, <1%)
	[M+45] <sup>+</sup> (329, 2%)
	[M+15] <sup>+</sup> (299, 15%)
	[M+13] <sup>+</sup> (297, <1%)
	[M+H] <sup>+</sup> (285, 100%)
	M <sup>+</sup> (284, 53%)
Purpurin (256)	[M-OH] <sup>+</sup> (267, 12%)
	[M+47] <sup>+</sup> (303, <1%)
	[M+45] <sup>+</sup> (301, 26%)
	[M+15] <sup>+</sup> (271, 3%)
	[M+13] <sup>+</sup> (269, 10%)
	[M+H] <sup>+</sup> (257, 100%)
	M <sup>+</sup> (256, <1%)
	[M-CO] <sup>+</sup> (228, 3%)

Anthraquinones were introduced to the ion source *via* a temperature controlled direct insertion probe (DIP). In order to obtain a good spectrum, a constant amount of sample must be introduced into GCQ, since the fluctuation of the concentration of the sample around the ion source might lead to the ionization process itself becoming unstable. Solutions for all anthraquinones were prepared in methanol at concentrations of  $3 \times 10^{-4}$  g/ml. One microliter samples of the solutions of anthraquinones ( $3 \times 10^{-7}$  g) were subjected to an evaporation step by a heater to eliminate the solvent. Each sample was then introduced to the ion source region of GCQ *via* a temperature controlled direct insertion probe (DIP). The range of temperature for heating was from 210°C to 370°C, and the speed of heating was 100°C/min. The ion injection time was 25 ms. Emodin and danthron were purchased from Sigma (Louis, MO). Purpurin, rhein and DME were obtained from Aldrich (Milwaukee, WI).

## Results and Discussion

Tables 1 and 2 list the results of DME CIMS of all anthraquinones at the reagent pressures of  $7.998 \times 10^{-2}$  and  $1.066 \times 10^{-2}$  Pa, respectively. Figures 2 and 3 show two typical spectra for DME CIMS of emodin at the pressures of  $1.066 \times 10^{-2}$  and  $7.998 \times 10^{-2}$  Pa, respectively. Table 1 shows the reagent pressure of  $7.998 \times 10^{-2}$  Pa, formation of the protonated ions (100%) and [M + 13]<sup>+</sup>, [M + 15]<sup>+</sup>, and [M + 45]<sup>+</sup> ions of all anthraquinones (5 to 42%). The formation of [M + 13]<sup>+</sup> adduct ions is *via* methylene reactions of *m/z* 45 followed by loss of one molecule of methanol, while the [M + 15]<sup>+</sup> ions are

Table 2 Ion-molecule reaction products of anthraquinones and dimethyl ether ions at  $1.066 \times 10^{-2}$  Pa

Compound (Mw)	Product ion ( <i>m/z</i> , relative intensity)
Emodin (270)	[M+47] <sup>+</sup> (317, <1%)
	[M+45] <sup>+</sup> (315, <1%)
	[M+13] <sup>+</sup> (283, 15%)
	[M+H] <sup>+</sup> (271, 47%)
	M <sup>+</sup> (270, 100%)
	[M-CO] <sup>+</sup> (242, 8%)
	[M-29] <sup>+</sup> (241, 21%)
	[M+H-CO-H <sub>2</sub> O] <sup>+</sup> (225, 16%)
	[M-29-CO] <sup>+</sup> (213, 33%)
	[M+H-2CO-H <sub>2</sub> O] <sup>+</sup> (197, 13%)
	[M-H <sub>2</sub> O-2CO] <sup>+</sup> (196, 12%)
	[M-29-2CO] <sup>+</sup> (185, 18%)
	[M-H <sub>2</sub> O-2CO-28] <sup>+</sup> (168, 16%)
	[M-29-2CO-28] <sup>+</sup> (157, 38%)
	[M-29-H <sub>2</sub> O-2CO-28] <sup>+</sup> (139, 11%)
Danthron (240)	[M-29-C <sub>2</sub> H <sub>2</sub> O-2CO-28] <sup>+</sup> (115, 10%)
	[M+47] <sup>+</sup> (287, <1%)
	[M+15] <sup>+</sup> (255, 3%)
	[M+H] <sup>+</sup> (241, 10%)
	M <sup>+</sup> (240, 30%)
	[M-CO] <sup>+</sup> (212, 24%)
	[M-2CO] <sup>+</sup> (184, 59%)
	[M-2CO-2x28] <sup>+</sup> (128, 100%)
	[M-71] <sup>+</sup> (169, 39%)
	[M-85] <sup>+</sup> (155, 45%)
	[M-H <sub>2</sub> O-2CO-28] <sup>+</sup> (138, 59%)
	[M+47] <sup>+</sup> (331, <1%)
	[M+45] <sup>+</sup> (329, <1%)
	[M+15] <sup>+</sup> (299, <1%)
	[M+13] <sup>+</sup> (297, <1%)
Rhein (284)	[M+H] <sup>+</sup> (285, 17%)
	M <sup>+</sup> (284, 100%)
	[M-OH] <sup>+</sup> (267, 15%)
	[M-CO] <sup>+</sup> (256, 40%)
	[M-OH-CO] <sup>+</sup> (239, 35%)
	[M-2CO] <sup>+</sup> (228, 35%)
	[M-OH-2CO] <sup>+</sup> (211, 23%)
	[M-OH-2CO-28] <sup>+</sup> (183, 21%)
	[M-OH-2CO-2x28] <sup>+</sup> (155, 29%)
Purpurin (256)	[M+47] <sup>+</sup> (303, <1%)
	[M+45] <sup>+</sup> (301, <1%)
	[M+15] <sup>+</sup> (271, <1%)
	[M+13] <sup>+</sup> (269, <1%)
	[M+H] <sup>+</sup> (257, 31%)
	M <sup>+</sup> (256, 100%)
	[M-CO] <sup>+</sup> (228, 58%)
	[M-H <sub>2</sub> O-CO-C <sub>2</sub> H <sub>2</sub> O] <sup>+</sup> (204, 13%)
	[M-CO-C <sub>2</sub> H <sub>2</sub> O] <sup>+</sup> (186, 22%)
	[M-2CO-C <sub>2</sub> H <sub>2</sub> O] <sup>+</sup> (158, 31%)
	[M-2CO-C <sub>2</sub> H <sub>2</sub> O-28] <sup>+</sup> (130, 53%)
	[M-2CO-C <sub>2</sub> H <sub>2</sub> O-2x28] <sup>+</sup> (102, 59%)
	[M-CO-3x28] <sup>+</sup> (144, 15%)
	[M-H <sub>2</sub> O-2CO-2x28] <sup>+</sup> (126, 87%)
	[M-141] <sup>+</sup> (115, 77%)

produced *via* a methyl addition reaction followed by loss of one molecule of formaldehyde. However, Table 2 shows that DME CIMS at  $1.066 \times 10^{-2}$  Pa, molecular ions of each anthraquinone appeared as the base peak for the M<sup>+</sup> ions of all anthraquinones except for danthron (30%). This is attributed to three reasons. First, if DME reagent gas is too low, ions may undergo direct electron impact (EI) to form M<sup>+</sup> ions and many fragment ions.<sup>25</sup> Second, anthraquinones may undergo charge exchange

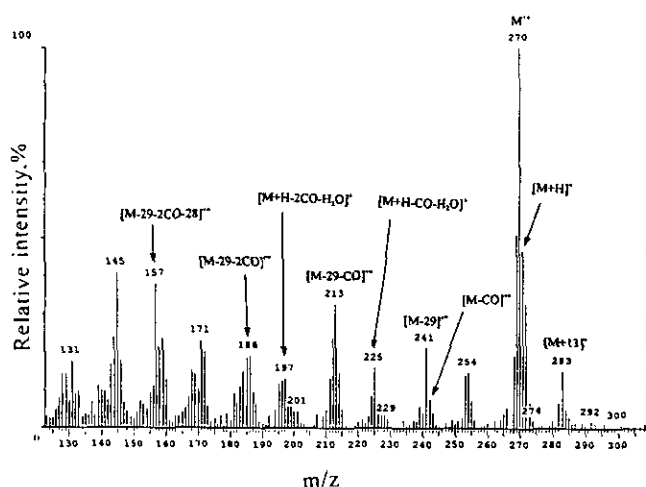


Fig. 2 Products of ion-molecule reactions of emodin with dimethyl ether at the pressure of  $1.066 \times 10^{-2}$  Pa.

reactions with either the molecular ion of DME ( $m/z$  46<sup>+</sup>,  $\text{CH}_3\text{OCH}_3^+$ ) or  $\text{He}^+$  ions to form  $\text{M}^+$  ions.<sup>1</sup> Third, the proton affinities of anthraquinones are close to that of the DME (207 kcal/mol).<sup>25</sup> In addition, the lower CI pressure conditions ( $1.066 \times 10^{-2}$  Pa) are also unfavorable for the formation of the ion/molecule products. The relative intensity of the  $[\text{M} + 13]^+$ ,  $[\text{M} + 15]^+$ ,  $[\text{M} + 45]^+$ ,  $[\text{M} + 47]^+$  ions of all anthraquinones was less than 3%, except for  $[\text{M} + 13]^+$  ions of emodin (15%). Comparing the results in Tables 1 and 2 indicates that higher pressure conditions cause preferential formation of the protonated ions and the ion/molecular reaction productions.

The reasons for observation of the DME pressure effect are discussed below. First, in the traditional ITMS, self-chemical ionizations were observed, typically<sup>26,27</sup> resulting in the formation of  $[\text{M} + \text{H}]^+$  ions. But in the GCQ, only the ion/molecule reaction products and DME reagent ions were allowed to enter the ion trap; all neutral molecules were left in the source region. Second, this pressure effect might be due to the short reaction times in the GCQ. Since the product ions were introduced into the analyzer by three lenses, ions were accelerated into the ion trap mass analyzer as soon as they formed, and only stayed in the ion source for a very short time. At the higher reagent pressure of  $7.998 \times 10^{-2}$  Pa, larger numbers of collisions might lead to the formation of the protonated ions and ion/molecular reaction products.

At the pressure of  $1.066 \times 10^{-2}$  Pa, many fragment ions were observed. These fragmentations were dissociated from either the molecular ions ( $\text{M}^+$ ) or protonated molecules ( $[\text{M} + \text{H}]^+$ ) of anthraquinones. Three reasons for this are discussed below. First, fragmentation might be due to the temperature effect of the ion source.<sup>23</sup> Second, it was due to the numbers of collisions when the ions traveled from the high-pressure source region (about  $1.333 \times 10^{-1}$  Pa) to the low-pressure trap region (about  $1.333 \times 10^{-4}$  Pa). Third, formation of the fragment ions was related to the kinetic energy of the ions and molecules in the CI source as discussed in regard to the ion trap detector (ITD).<sup>25</sup> Since the product ions were accelerated into the ion trap mass analyzer by three lenses, the ions obtained more kinetic energy during the acceleration. Therefore, the product ions might have dissociated into many fragment ions during the process of acceleration. At the pressure of  $7.998 \times 10^{-2}$  Pa, the kinetic energy of ions in the source region can be more effectively collision-cooled (deactivated) by the DME.<sup>25</sup> From our study in

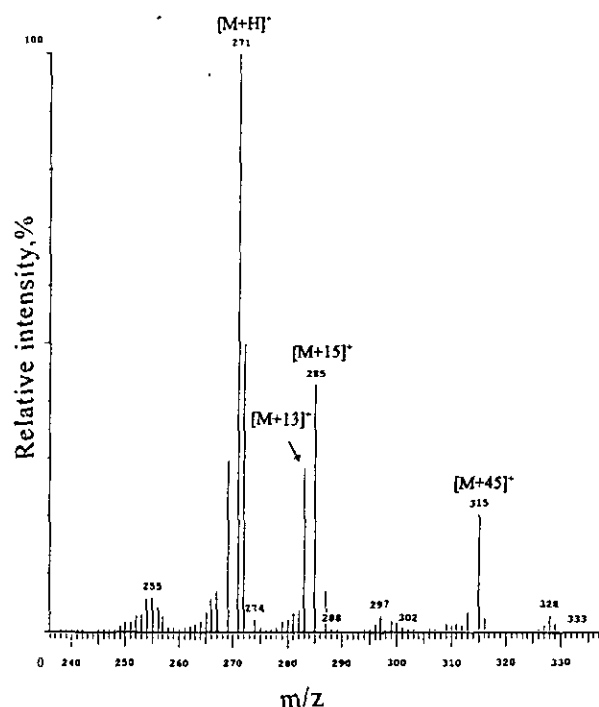


Fig. 3 Products of ion-molecule reactions of emodin with dimethyl ether at the pressure of  $7.998 \times 10^{-2}$  Pa.

GCQ, the standard operating pressure for EI mode of GCQ is from  $3.999 \times 10^{-3}$  to  $6.665 \times 10^{-3}$  Pa typically, while the best pressure range for CIMS in GCQ is approximately from  $3.999 \times 10^{-2}$  to  $7.998 \times 10^{-2}$  Pa typically for the series of ion-molecule reactions we have examined. These include anthraquinones, tricyclic antidepressants, flavones, flavanones and dibenzo-18-crown-6 with dimethyl ether. All compounds we have examined have shown similar results toward the DME pressure effects, except for the dopamine and adrenaline.<sup>23</sup> For these two compounds, nice ion/molecule reaction products and protonated molecules could be obtained even at the low DME pressure of  $1.066 \times 10^{-2}$  Pa. The reason for this might be that these compounds are very basic and possess high proton affinity in the gas-phase.

## Conclusion

It is true that with the external chemical ionization configuration of GCQ, the space charge effect and self chemical ionization during ion/molecule reactions in the ITMS can be avoided, and the reproducibility, sensitivity and resolution in the GCQ can be improved. However, the reagent pressure of DME must be controlled very carefully for anthraquinones in order to obtain nice CIMS spectra in GCQ. Since the pressure effect in GCQ is notable within a very small range of pressures for many compounds, this information is important to draw the attention of those using the ion trap with an external source.

## Acknowledgements

Grants supporting this work from the National Science Council of the Republic of China (Grant No. NSC 89-2113-M-032-024) are gratefully acknowledged.

## References

1. J. S. Brodbelt, J. N. Louris, and R. G. Cooks, *Anal. Chem.*, **1987**, *59*, 1278.
  2. C.-C. Liou, J. Isbell, H.-F. Wu, J. S. Brodbelt, R. A. Bartsch, J. C. Lee, and J. L. Hallman, *J. Mass Spectrom.*, **1995**, *30*, 572.
  3. J. Brodbelt, C.-C. Liou, and T. Donovan, *Anal. Chem.*, **1991**, *63*, 1205.
  4. T. Donovan and J. Brodbelt, *Org. Mass Spectrom.*, **1992**, *27*, 9.
  5. T. Donovan, C.-C. Liou, and J. Brodbelt, *J. Am. Soc. Mass Spectrom.*, **1992**, *3*, 39.
  6. T. Donovan and J. Brodbelt, *J. Am. Soc. Mass Spectrom.*, **1992**, *3*, 47.
  7. C.-C. Liou, E. S. Eichmann, and J. S. Brodbelt, *Org. Mass Spectrom.*, **1992**, *27*, 1098.
  8. T. Donovan and J. Brodbelt, *Biol. Mass Spectrom.*, **1992**, *21*, 254.
  9. T. D. McCarley and J. Brodbelt, *Anal. Chem.*, **1993**, *65*, 2380.
  10. E. S. Eichmann and J. S. Brodbelt, *Org. Mass Spectrom.*, **1993**, *28*, 665.
  11. E. S. Eichmann and J. S. Brodbelt, *Org. Mass Spectrom.*, **1993**, *28*, 737.
  12. A. Colorado and J. Brodbelt, *Anal. Chem.*, **1994**, *66*, 2330.
  13. G. F. Bauerle, Jr., B. J. Hall, N. V. Tran, and J. S. Brodbelt, *J. Am. Soc. Mass Spectrom.*, **1995**, *7*, 250.
  14. G. F. Bauerle, Jr., and J. S. Brodbelt, *J. Am. Soc. Mass Spectrom.*, **1995**, *6*, 627.
  15. E. J. Alvarez and J. S. Brodbelt, *J. Mass Spectrom.*, **1995**, *30*, 625.
  16. M. Tang, J. Isbell, B. Hodges, and J. Brodbelt, *J. Mass Spectrom.*, **1995**, *30*, 977.
  17. J. Isbell and J. S. Brodbelt, *J. Am. Soc. Mass Spectrom.*, **1996**, *7*, 565.
  18. E. J. Alvarez and J. S. Brodbelt, *J. Mass Spectrom.*, **1996**, *31*, 901.
  19. J. X. Shen and J. Brodbelt, *J. Mass Spectrom.*, **1996**, *31*, 1389.
  20. J. S. Brodbelt, *Mass Spectrom. Rev.*, **1997**, *16*, 91.
  21. A. A. Mosi, R. H. Skelton, and G. K. Eigendorf, *J. Mass Spectrom.*, **1999**, *34*, 1274.
  22. H.-F. Wu and Y.-P. Lin, *J. Mass Spectrom.*, **1999**, *34*, 1283.
  23. H.-F. Wu and Y.-P. Lin, *Eur. Mass Spectrom.*, **2000**, *6*, 65.
  24. H.-F. Wu, *J. Mass Spectrom.*, **2000**, *35*, 1049.
  25. R. C. Dorey, *Org. Mass Spectrom.*, **1989**, *24*, 973.
  26. J. W. Eichelberger, W. L. Budde, and L. E. Slivon, *Anal. Chem.*, **1987**, *59*, 2730.
  27. S. A. McLuckey, G. L. Glish, K. G. Asano, and G. J. Van Berkel, *Anal. Chem.*, **1988**, *60*, 2312.
-

(3)

## Simulation of the collisional cooling effect for binary and ternary buffer gas mixtures in a quadrupole ion trap mass spectrometer

Hui-Fen Wu,\* Li-Wei Chen, Jhen-Chen Wang<sup>a</sup> and Ya-Ping Lin

Department of Chemistry, Tamkang University, Tamsui, Taipei Hsien, 25137, Taiwan, ROC

Reprinted from

*European Journal of Mass Spectrometry* 7:1-6 (2001)

© IM Publications 2001

IM Publications, 6 Charlton Mill, Charlton, Chichester, West Sussex PO18 0HY, United Kingdom.

Tel: +44 (0) 1243-811334 Fax: +44 (0) 1243-811711, E-mail: [ems@impub.demon.co.uk](mailto:ems@impub.demon.co.uk),

URL: <http://www.impub.co.uk>.

## Simulation of the collisional cooling effect for binary and ternary buffer gas mixtures in a quadrupole ion trap mass spectrometer

Hui-Fen Wu,<sup>\*</sup> Li-Wei Chen, Jhen-Chen Wang<sup>a</sup> and Ya-Ping Lin

Department of Chemistry, Tamkang University, Tamsui, Taipei Hsien, 25137, Taiwan, ROC

Simulation of the collisional cooling effect using binary and ternary buffer gas mixtures in the ion trap mass spectrometer was performed using the SIMION 6.0 program, in which a 3D collision model was used to describe the ion–buffer gas collisions. Computation of the ion kinetic energy based on the Langevin theory under various conditions was used to account for the effects of mixed buffer gases on ion–collisional cooling. The addition of small amounts (8–9%) of one or two heavier target gases (nitrogen, argon or SF<sub>6</sub>) to the 1 mtorr helium buffer gas in the ion trap can greatly improve the collisional cooling effects. The kinetic energy of ions can be reduced to close to 0 eV. Although the use of ternary buffer gas mixtures can also effectively improve the collisional cooling effects, the use of binary buffer gas mixtures is the better choice due to convenience and lower cost in real ion trap applications.

**Keywords:** quadrupole ion trap mass spectrometer, collisional cooling effect, buffer gas mixtures, simulation

### Introduction

The ion trap mass spectrometer (ITMS) has been widely used in many applications<sup>1–4</sup> owing to its low cost, high sensitivity and tandem mass spectrometry capability.<sup>5–7</sup> Studies of the cooling phenomenon using various ion trap methods have been discussed.<sup>8–11</sup> Among these methods, collisional cooling for ions in the ion trap by using a buffer gas is a very efficient method.<sup>12–17</sup> The existence of the buffer gas in the ITMS is very important because ion collisions with the neutral buffer gas lead to the reductions in ion velocity, trajectory amplitude and kinetic energy. Thus, the sensitivity and resolution of the ITMS can be greatly enhanced.<sup>18</sup> The use of buffer gases other than He has been reported.<sup>19–24</sup> Morand *et al.* found that some heavier target gases, when added in small amounts to the He buffer gas in the ion trap, can improve the trapping efficiency and the internal energy deposition during collisionally-activated dissociation (CAD).<sup>23</sup> A number of simulations of the ion trap mass spectrometer have been reported.<sup>25–38</sup> We used a simulation method to investigate the ion–collisional damping effect on ions as a function of different parameters including ion mass, temperature, ion trap electrode size, pressure and the use of alternative buffer gases.<sup>38</sup> In general, 1 mtorr of He is typi-

cally used for the ITMS. In this study, we attempted to develop a more effective buffer gas mixture in the ITMS by adding a very small amount of a second buffer gas component to the standard 1 mtorr buffer gas to improve the ion trap resolution.

### Computational methods

In this study, the SIMION 6.0 program<sup>39</sup> in combination with the Langevin collision theory was used to perform all simulations. The real geometry of the standard Finnigan ion trap electrodes was used in the simulation. The ion trap electrode internal surface curve was created using a geometry file provided by the SIMION 6.0 program. The physical parameters of the ITMS are described in the following. The electron ionization source voltage was 70 eV. The initial ion kinetic energy in the source region was 0 eV. The number of ions was 50. The operational ion trap RF frequency was  $1.1 \times 10^6$  Hz. The ion mass was 200 amu,  $q_z = 0.5$ ,  $a_z = 0$ ,  $z_0 = 0.707$  cm and  $r_0 = 1.0$  cm. The RF potential on the ring electrode was controlled by user-written programs and the potential applied to the ring electrode was given by  $V_{RF} = U + V \cos(2\pi\Omega t + \beta_0)$ , where  $V$  is the maximum amplitude of the RF voltage,  $U$  is the DC voltage (set as 0 V),  $\Omega$  is the RF frequency (1.1 MHz),  $t$  is the ion flight

<sup>\*</sup>Current address: Department of Electronic Engineering, Tung-Nan Institute of Technology

time and  $\beta_0$  is the initial RF phase. The RF voltage used was 100 V (zero-to-peak). DC voltage was applied to eject the ions out of the trap for detection.

The simulations were performed on an IBM PC computer (Pentium 166 MHz, 32 MB). The items used for computation included ion number, velocity and kinetic energy. The recording time was estimated from the time when ions were generated in the ion trap to the time when ions were ejected to the detector. In order to apply the Langevin theory to the program, a series of programs and equations were written into the original user programs (inject.prg and trap.prg) using the RPN Language to perform simulations. For example, the collisional probability was altered to relate to the conditions obtained by mixing two or three kinds of buffer gas. The buffer gas mass was set to 4, 28, 40 and 146 mass units for helium, nitrogen, argon and  $\text{SF}_6$  buffer gases, respectively. The buffer gas collisions with the ions were assumed to be elastic collisions. The initial velocity of the buffer gas was set at zero, then the collisional probability was calculated from Equation 1.<sup>40,41</sup> According to the Langevin theory,<sup>42</sup> the collision cross-section ( $\sigma$ ) for a singly-charged ion colliding with a buffer gas can be expressed as in Equation 1:

$$\sigma = \pi b_0^2 = (2\pi e / 4\pi\epsilon_0 v) \times (\alpha_e / \mu)^{1/2} \quad (1)$$

where  $\epsilon_0$  is the permittivity of free space,  $\mu$  is the reduced mass of the collision system,  $v$  is the relative velocity of the collision partners,  $e$  is the charge and  $\alpha_e$  is the electronic polarizability of the buffer gas. The probability of collision per unit of time can be represented as in Equation 2:

$$P = nv\sigma \quad (2)$$

where  $n$  is the number density of collision-gas atoms and  $P$  is the collisional probability. Combining Equations 1 and 2 to calculate the collisional probability gives Equation 3:<sup>41</sup>

$$P = (e / 2\epsilon_0) \times (\alpha_e / \mu)^{1/2} \times (p / kT) \quad (3)$$

where  $p$ ,  $T$  and  $k$  represent pressure, temperature and the Boltzmann constant, respectively. When the collisional probabilities for mixtures of two or three buffer gases were calculated, the collisional probability for each buffer gas was calculated individually. In the ITMS, the presence of the buffer gas damps the ion trajectories toward the center of the ion trap by reducing the ion kinetic energies.<sup>18</sup> Thus, calculating the ion kinetic energy values can be used to represent the collisional cooling effect. The simulation used head-on collisions and discontinuous collision models for ions colliding with a buffer gas. No consideration of different scattering angles or the conversion of axial kinetic energy to radial kinetic energy was used. After collision, it was assumed that the ion movement directions were not changed and that only the ion kinetic energy was decreased. The kinetic energy of an ion just after one collision is given by  $[(m_{\text{ion}} - m_{\text{buffer}}) / (m_{\text{ion}} + m_{\text{buffer}})]^2 \times KE$  eV, where  $KE$  represents the kinetic energy of the ion just before the collision. For all experiments performed in this simulation, 50 ions of  $m/z$  200

were used in all calculations to obtain statistical results from the user program. All ions were assumed to be positively and singly charged. The simulation neglected the ion-ion repulsion effect. Although it can be approximately calculated using the SIMION 6.0 program, the space charge effect would not occur since only a small number of ions were considered.

The software package used in this study was SIMION 3D (Version 6.0) developed by the Lockheed Idaho Technologies Company.<sup>39</sup> The Langevin collision theory was written into the SIMION program to model the simulation experiments. The equation  $P' = 1 - e^{-P\Delta t}$  was used to calculate the collision. The trap.prg user program was used to demonstrate the motions of the 50 ions in the ion trap. The inject.prg user program was used to demonstrate the collision gas effect (simulated by the mean-free-path collisional cooling model). The mean free path was set at 1 mm, the random time of birth = 0.909091  $\mu\text{s}$  and the ion time step = 0.1  $\mu\text{s}$ . Fifty ions were produced in groups at the same time and at the same positions ( $x = 40$ ,  $y = 0$  and  $z = 0$ ).

Random collisions were computed using the following procedures in the simulation program.

- (1) Enter temperature, pressure and buffer gas mass values. Use these parameters to calculate the collisional probability as  $P = (e / 2\epsilon_0) \times (\alpha_e / \mu)^{1/2} \times (p / kT)$ .
- (2) Calculate the collisional probability using  $P' = 1 - e^{-P\Delta t}$ , where  $d$  is equal to the product of the ion time-step and the ion velocity and  $f$  is the mean free path.<sup>39</sup>
- (3) Generate a random number for each time step. The value for the random number is between 0 and 1.
- (4) Compare the probability for collision during each time step with the random number. If the probability of collision is larger than the random number, then a collision will occur.
- (5) Calculate the reduction factor for the ion final velocity after collision as  $(m_{\text{ion}} - m_{\text{buffer}}) / (m_{\text{ion}} + m_{\text{buffer}})$ , where  $m_{\text{ion}}$  represents the ion mass, and  $m_{\text{buffer}}$  represents the mass of the buffer gas.<sup>25</sup>
- (6) Multiply the original velocity of the ion by the reduction factor  $(m_{\text{ion}} - m_{\text{buffer}}) / (m_{\text{ion}} + m_{\text{buffer}})$  to give a new value. Store this value as the new ion velocity.
- (7) Transform the new ion velocity into a three-dimensional velocity in order to calculate the final kinetic energy.
- (8) For simulation of the conditions using only one buffer gas, store the new ion velocity after collision in order to calculate the new kinetic energy.
- (9) When calculating the conditions using mixtures of two or three buffer gases, regardless of whether the ions will collide with the first kind of buffer gas or not, return the procedure to step (4) in order to calculate the probability of collision of the ions with the second buffer gas.
- (10) Apply the various random numbers generated in step (3) to different kinds of buffer gases.
- (11) Average the kinetic energies of the 50 ions after the ions reach the detector.

With a knowledge of computer organization and programming basics, the number of random numbers actually

generated throughout one trial of the simulation running in the program can be calculated as illustrated below. The Pentium-166 MHz computer used for the simulation in this study has a well-designed CPU/FPU (central processing unit / floating point unit) capability which can process each simple integer instruction or simple floating-point instruction in one clock-cycle time; for 166 MHz, the clock cycle is 0.006  $\mu$ s. In this study, the simulation program generates the random number by calling the random number generation function offered by the simulation language compiler, and then compares the random number with the collision probability ( $P'$ ) which had been calculated beforehand in the program. This iteration of random number generation and comparison continues until the collision probability ( $P'$ ) is larger than the random number. After examination of the CPU/FPU instruction codes created by the compiler for the complicated function used for random number generation, the time for each iteration can be reasonably estimated as 100 clock cycles, or 0.6  $\mu$ s. Note that this estimation has taken consideration of the Pentium architecture which highlights the super-scalar/super-pipelined and level-1/level-2 cached structure. For our simulation to reach the condition where the collision probability ( $P'$ ) is larger than the generated random number, usually takes five minutes (300 s) for one trial run of the simulation. Therefore, the total number of 0.6  $\mu$ s-long iterations in 300 s is  $5 \times 10^8$ . This sufficiently large number of iterations definitely implies that the random collision simulation would approximate the Gaussian distribution model. Further, the simulation program defines the modulus of the random generator as a 32-bit integer type, which means the maximum number of iterations is  $4 \times 10^9$  or 40 min at the most during the running of the simulation. In conclusion, the period of the random collision in this simulation has generated a sufficiently long sequence of random numbers to warrant its correctness.

## Results and discussion

In this study, a simulation was performed using SIMION software<sup>39</sup> to calculate the kinetic energy of the ions. Collisions between the ions and the buffer gas lead to a reduction in the velocity, kinetic energy and trajectory amplitude of the ions inside the ITMS. As a result, ions gather in the center of the ion trap leading to a reduction in size of the ion cloud. When ions are ejected through the opposite end cap to the electron multiplier for detection, most of these ions can be detected. However, without the buffer gas in the ion trap, the ions oscillate with a rather large amplitude due to the RF trapping potential in the ion trap.

In order to examine the collisional cooling effect for different mixtures of buffer gases, the following simulation experiments were performed: 1 mtorr of the main component of the buffer gas mixture together with a very small amount (0.01–0.09 mtorr) of the second buffer gas in the ion trap with 50 ions of  $m/z$  200. The results are shown in Fig-

ures 1–4. Figure 1 shows a comparison of the average kinetic energy variation as a function of the total pressure of various binary buffer gas mixtures: in this case from the addition of 0.01–0.09 mtorr of nitrogen, argon or  $\text{SF}_6$  to the 1 mtorr of helium buffer gas in the ion trap. The kinetic energies of the ions in all three buffer gas mixtures, in this case those with nitrogen (indicated by the line with the solid square mark), argon (indicated by the line with the solid triangle mark) and  $\text{SF}_6$  (indicated by the line with the open circle mark) were reduced by the addition of a very small amount of the second buffer gas. Also, the average kinetic energy of all ions was effectively reduced as the pressure of the second buffer gas was increased from 0.01 to 0.09 mtorr (the total gas pressure increased from 1.01 to 1.09 mtorr). Moreover, when the additional pressure from the second buffer gas reached 0.08–0.09 mtorr (total pressure 1.08–1.09 mtorr), the average kinetic energies of all of the ions in all buffer gas mixtures had been reduced to close to 0 eV.

In order to observe the effect of adding a second heavier target gas, the standard condition of using a single buffer gas (He) is also shown in Figure 1 (indicated by the line with the solid circle mark). The ion kinetic energy in pure He gas fluctuated between 40 and 50 eV. Thus, a reduction of more than 40 eV of ion kinetic energy, resulting from the addition of a very small amount of heavier buffer gas into the ITMS, was observed. In the simulation, ions were injected into the ion trap with a fixed kinetic energy through the hole in one endcap of the ion trap and were recorded on reaching the detector. Because of the high ion kinetic energy (approximately 45 eV) with only a single buffer gas, only a few ions would be trapped upon injection at this kinetic energy; the ions would rather proceed straight across the ion trap. However, using binary buffer gas mixtures, the ion kinetic energy is reduced to close to 0 eV. The reasons for this behavior are as follows. First, since the RF field constantly accelerates and decelerates the ions, the introduction of a buffer gas gradually decreases the amplitude of oscillation (related to kinetic energy) of any ion over time. Second, the average

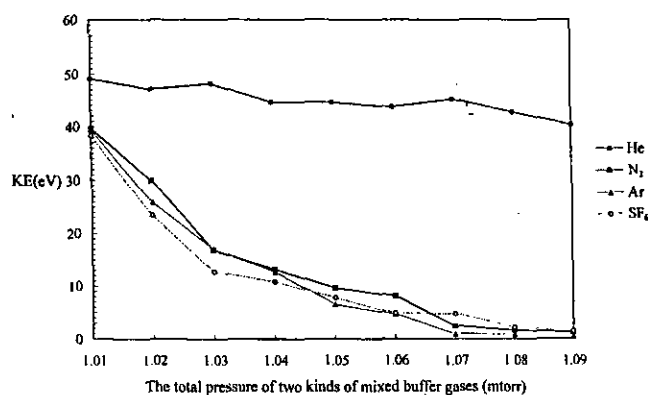


Figure 1. Comparison of the kinetic energy variation as a function of the total pressure of two mixed buffer gases. Addition of small amounts (0.01–0.09 mtorr) of nitrogen, argon or  $\text{SF}_6$  to the 1 mtorr helium buffer gas in the ion trap for 50 ions of  $m/z$  200 (temperature = 375 K,  $q_z = 0.5$ ).



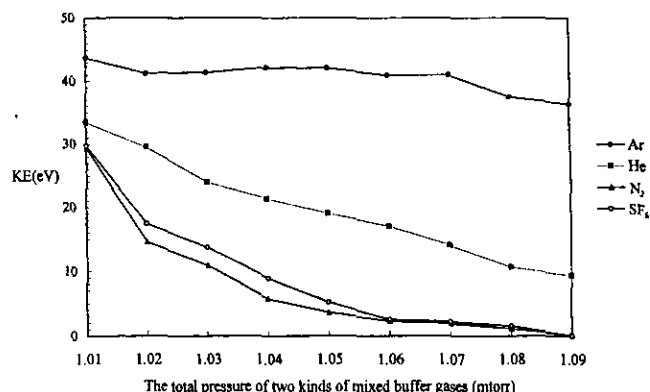


Figure 2. Comparison of the kinetic energy variation as a function of the total pressure of two mixed buffer gases. Addition of small amounts (0.01–0.09 mtorr) of helium, nitrogen or  $\text{SF}_6$  to the 1 mtorr argon buffer gas in the ion trap for 50 ions of  $m/z$  200 (temperature = 375 K,  $q_z = 0.5$ ).

energy exchanged per collision depends on the reduced mass of the ion and target. Third, from Equation 3 we know that the collisional probability is proportional to the pressure of the buffer gas. Thus, as the pressure increases, the amount of buffer gas inside the ion trap increases. As a result, the collisional probability is larger and the ion kinetic energy can be reduced after collisional cooling by the buffer gases.

Figures 2 to 4 show data obtained using a heavier gas as the main (1 mtorr) component of the buffer gas and compare the use of nitrogen, Ar or  $\text{SF}_6$  against helium as the main component of the buffer gas together with a very small amount of an added second buffer gas in each case. For the data in these figures, the simulation experiments were performed under exactly the same conditions as in Figure 1, except that different combinations of buffer gases were used. The use of single buffer gases (1 mtorr of Ar, nitrogen or  $\text{SF}_6$  gas, indicated by the line with the solid circle mark plotted from 1.01 to 1.09 mtorr) is compared in Figures 2–4. The ion kinetic energy in pure Ar, nitrogen or  $\text{SF}_6$  gas fluctuates between 40 and 45 eV, so that replacing 1 mtorr of He buffer gas with Ar, nitrogen or  $\text{SF}_6$  leads to similar results, as shown in Figures 2–4. Thus, we conclude that the collisional cooling effect is efficiently improved with an increase in pressure of a second buffer gas component. When Ar (Figure 2), nitrogen (Figure 3) or  $\text{SF}_6$  (Figure 4) were used as the 1 mtorr main buffer gas and He buffer gas was added in small amounts to this main component, the reduction in ion kinetic energy was not as pronounced as with the addition of nitrogen, Ar or  $\text{SF}_6$ . Only a small percentage of a heavy gas damps the kinetic energy down to close to zero as shown in Figure 1. This is predominately due to the mass effect. However, because the mass of He is much lower than that of Ar, nitrogen or  $\text{SF}_6$ , the addition of He as a second buffer gas does not reduce the kinetic energy down to 0 eV (see Figures 2–4). Thus, we know that using He as the second, minor buffer gas component is the worst choice, since this buffer gas mixture reduces the ion kinetic energy the least. Figures 2–4 also

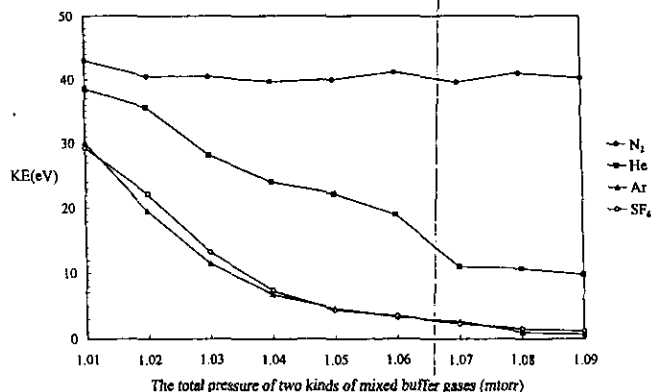


Figure 3. Comparison of the kinetic energy variation as a function of the total pressure of two mixed buffer gases. Addition of small amounts (0.01–0.09 mtorr) of helium, argon or  $\text{SF}_6$  to the 1 mtorr nitrogen buffer gas in the ion trap for 50 ions of  $m/z$  200 (temperature = 375 K,  $q_z = 0.5$ ).

indicate that the addition of He as a second buffer gas provides a better cooling effect than the use of a pure, heavier buffer gas such as Ar, nitrogen or  $\text{SF}_6$ . The most likely reason is that the collision probability for the mixed buffer gas is larger than that for a pure buffer gas. Collisions with the lower mass atoms (He) typically result in less scattering in the ion trajectory than do collisions with higher mass atoms (Ar,  $\text{N}_2$  or  $\text{SF}_6$ ). A higher degree of scattering can lead to a decrease in the ion trap performance, such as resolution and sensitivity.

The collisional cooling effect from using a mixture of three buffer gases was also examined. In order to check whether using three kinds of buffer gas is better than using two, similar methods were applied to calculate the ion kinetic energies as detailed above for the binary buffer gas mixtures except for the addition of very small and equal amounts of two additional buffer gases into the 1 mtorr main buffer gas. Figure 5 shows the average kinetic energy varia-

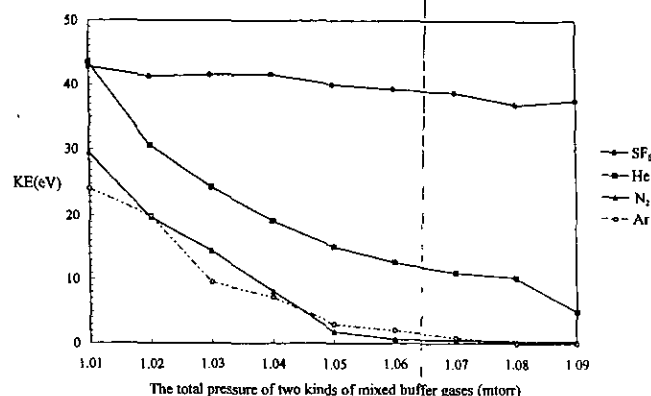


Figure 4. Comparison of the kinetic energy variation as a function of the total pressure of two mixed buffer gases. Addition of small amounts (0.01–0.09 mtorr) of helium, nitrogen or argon to the 1 mtorr  $\text{SF}_6$  buffer gas in the ion trap for 50 ions of  $m/z$  200 (temperature = 375 K,  $q_z = 0.5$ ).

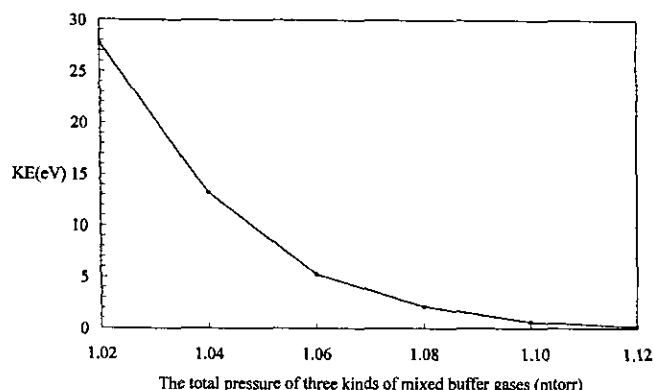


Figure 5. The average kinetic energy variation as a function of the total pressure of three mixed buffer gases. Addition of equal and small amounts (0.01–0.06 mtorr) of nitrogen and argon to the 1 mtorr helium buffer gas in the ion trap for 50 ions of  $m/z$  200 (temperature = 375 K,  $q_z = 0.5$ ).

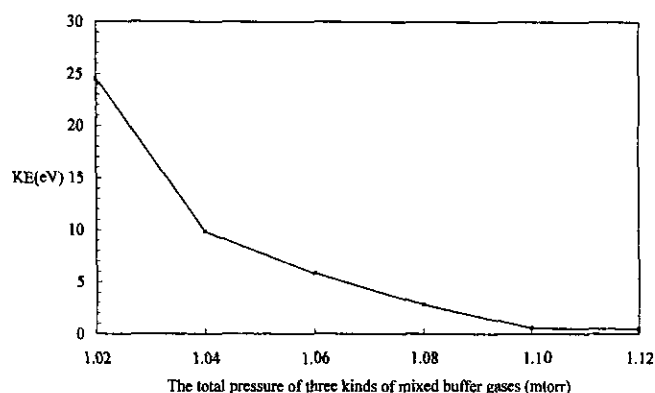


Figure 6. Kinetic energy variation as a function of the total pressure of three mixed buffer gases. Addition of equal and small amounts (0.01–0.06 mtorr) of helium and  $\text{SF}_6$  to the 1 mtorr argon buffer gas in the ion trap for 50 ions of  $m/z$  200 (temperature = 375 K,  $q_z = 0.5$ ).

tion as a function of the total pressure from a ternary buffer gas mixture. Equal and small amounts (0.01–0.06 mtorr) of nitrogen and Ar were added to the 1 mtorr helium buffer gas in the ion trap. The initial ion kinetic energy at a total pressure of 1.02 mtorr was 27.74 eV. However, as the additional amount of both Ar and nitrogen gas reached 0.06 mtorr (total pressure = 1.12 mtorr), the ion kinetic energies were reduced to close to 0 eV. If we compare Figure 5 with Figure 1, when 0.06 mtorr of nitrogen or Ar was added to 1 mtorr He (total pressure = 1.06 mtorr), the ion kinetic energies were 8.09 and 4.66 eV, whereas in Figure 5 (total pressure again = 1.06 mtorr) the ion kinetic energy was 5.27 eV. This result indicates that the use of a mixture of three buffer gases is no better than the use of two buffer gases. Figure 6 shows the kinetic energy variation as a function of the total pressure for a ternary buffer gas mixture using 1 mtorr of Ar as the main buffer gas component. Thus, by adding equal and small amounts (0.01–0.06 mtorr) of helium and  $\text{SF}_6$  to the 1 mtorr argon buffer gas in the ion trap, the results in Figure 6 are very similar to the results shown in Figure 5. Therefore, there is no difference in the collisional cooling effect obtained by using different combinations of buffer gases in a ternary gas mixture. Although the use of three buffer gases can also effectively improve the collisional cooling effect, the result was not statistically better than the use of a binary buffer gas mixture. In real ion trap applications, the use of two buffer gases is the best choice based on convenience and cost.

## Conclusion

This simulation study describes the use of mixed buffer gases, consisting of two or more components, in an ion trap. Mixed buffer gases greatly reduce the average kinetic energy and improve the ion-collisional cooling effects.

These results provide novel insights for improving the resolution and sensitivity of ion trap mass spectrometry.

## Acknowledgments

We wish to acknowledge the financial support of the National Science Council of the Republic of China (Grant No. NSC 89-2113-M-032-024).

## References

1. H.-F. Wu and J.S. Brodbelt, *J. Am. Chem. Soc.* **116**, 6418 (1994).
2. H.-F. Wu and J.S. Brodbelt, *J. Am. Soc. Mass Spectrom.* **4**, 718 (1993).
3. H.-F. Wu and J.S. Brodbelt, *Inorg. Chem.* **34**, 615 (1995).
4. H.-F. Wu and J.S. Brodbelt, *J. Includ. Phenom.* **18**, 37 (1994).
5. J.N. Louris, R.G. Cooks, J.E.P. Syka, P.E. Kelly, G.C. Stafford, Jr and J.F.J. Todd, *Anal. Chem.* **59**, 1677 (1987).
6. J.N. Louris, J.S. Brodbelt, R.G. Cooks, G.C. Glish, G.J.V. Berkel and S.A. McLuckey, *Int. J. Mass Spectrom. Ion Processes* **96**, 117 (1990).
7. J.S. Brodbelt and R.G. Cooks, *Spectra* **11**, 30 (1988).
8. I. Siemers, R. Blatt, T. Sauter and W. Neuhauser, *Phys. Rev. A* **38**, 5121 (1988).
9. R. Blümel, C. Kappler, W. Quint and H. Walther, *Phys. Rev. A* **40**, 808 (1989).
10. D.A. Church and H.G. Dehmelt, *J. Appl. Phys.* **40**, 3421 (1969).
11. F. Diedrich, E. Peik, J.M. Chen, W. Quint and H. Walther, *Phys. Rev. Lett.* **59**, 2931 (1987).
12. R.E. March, F.A. Londry, S. Fontana, S. Catinella and P. Traldi, *Rapid Commun. Mass Spectrom.* **7**, 929 (1993).

13. L.S. Cutler, R.P. Giffard and M.D. McGuire, *Appl. Phys.* **B36**, 137 (1985).
14. C. Basic, J.R. Eyler and R.A. Yost, *J. Am. Soc. Mass Spectrom.* **3**, 716 (1992).
15. P. Liere, V. Steiner, K.R. Jennings, R.E. March and J.-C. Tabet, *Int. J. Mass Spectrom. Ion Phys.* **167/168**, 735 (1997).
16. Y. Moriwaki, M. Tachikawa and T. Shimizu, *Jpn J. Appl. Phys.* **35**, 757 (1996).
17. M. Splendore, F.A. Londry, R.E. March, R.J.S. Morrison, P. Perrier and J. Andre, *Int. J. Mass Spectrom. Ion Processes* **156**, 11 (1996).
18. H.-F. Wu and J.S. Brodbelt, *Int. J. Mass Spectrom. Ion Processes* **115**, 67 (1992).
19. K.L. Schey, H.I. Kenttamaa, V.H. Wysocki and R.G. Cooks, *Int. J. Mass Spectrom. Ion Processes* **90**, 71 (1989).
20. J.A. Nystrom, M.M. Bursey and J.R. Hass, *Int. J. Mass Spectrom. Ion Processes* **55**, 263 (1983/1984).
21. M.M. Bursey, J.A. Nystrom and J.R. Hass, *Anal. Chim. Acta* **159**, 275 (1984).
22. M.M. Bursey, J.A. Nystrom and J.R. Hass, *Anal. Chim. Acta* **159**, 265 (1984).
23. K.L. Morand, K.A. Cox and R.G. Cooks, *Rapid Commun. Mass Spectrom.* **6**, 520 (1992).
24. S.A. Lammert and J.M. Wells, *Rapid Commun. Mass Spectrom.* **10**, 361 (1996).
25. H.P. Reiser, R.K. Julian and R.G. Cooks, *Int. J. Mass Spectrom. Ion Processes* **121**, 49 (1992).
26. F.-S. Huang and R.C. Dunbar, *J. Am. Chem. Soc.* **111**, 6497 (1989).
27. F. Vedel, J. Andre, M. Vedel and G. Brincourt, *Phys. Rev.* **A27**, 2321 (1983).
28. F. Vedel and J. Andre, *Phys. Rev.* **A29**, 2098 (1984).
29. J. Andre and J.P. Schermann, *Phys. Lett.* **45A**, 139 (1973).
30. F. Vedel, and J. Andre, *Int. J. Mass Spectrom. Ion Processes* **65**, 1 (1985).
31. J.H. Parks and A. Szoke, *J. Chem. Phys.* **103**, 1422 (1995).
32. R.E. March, M.R. Weir, M. Tkaczyk, F.A. Londry, R.L. Alfred, A.M. Franklin and J.F.J. Todd, *Org. Mass Spectrom.* **28**, 499 (1993).
33. F.A. Londry, R.L. Alfred and R.E. March, *J. Am. Soc. Mass Spectrom.* **4**, 687 (1993).
34. L. He and D.M. Lubman, *Rapid Commun. Mass Spectrom.* **11**, 1467 (1997).
35. U. Wilhelm, C. Weickhardt and J. Grotemeyer, *Rapid Commun. Mass Spectrom.* **10**, 473 (1996).
36. V.M. Doroshenko and R.J. Cotter, *J. Mass Spectrom.* **31**, 602 (1997).
37. C. Weil, M. Nappi, C.D. Cleven, H. Wollnik and R.G. Cooks, *Rapid Commun. Mass Spectrom.* **10**, 742 (1996).
38. H.-F. Wu, L.-W. Chen and Y.-P. Lin, *J. Chin. Chem. Soc.* **46**, 923 (1999).
39. D.A. Dahl, Idaho National Engineering Laboratory, Idaho Falls, ID, USA, Version 6.0 (1995).
40. R.E. March and J.F.J. Todd, *Practical Aspects of Ion Trap Mass Spectrometry*, Vol. 1. CRC Press, Boca Raton, FL, USA (1995).
41. T. Su and M.T. Bower, *J. Chem. Phys.* **58**, 3027 (1973).
42. G. Gioumoussis and D.P. Stevenson, *J. Chem. Phys.* **29**, 294 (1958).

Received: 24 February 2000

Revised: 19 June 2000, 23 August 2000, 26 October 2000

Accepted: 6 November 2000

Web Publication: 16 February 2001

## (4) JMS Letters

Dear Sir,

### Determination of the Sensitivity of an External Source Ion Trap Tandem Mass Spectrometer Using Dimethyl Ether Chemical Ionization

Tandem mass spectrometry is a rapid and powerful analytical technique that can provide trace mixture analysis and structure elucidation. The ion trap mass spectrometer has been widely used since it became commercially available in 1983. The reason is attributed to its tandem mass capability.

Within the last decade, a number of studies of ion–molecule reactions of dimethyl ether (DME) ions in the ion trap mass spectrometer have been published by Brodbelt and co-workers.<sup>1,2</sup> Two main reagent ions, of  $m/z$  45 ( $\text{CH}_3\text{O}=\text{CH}_2^+$ ) and 47 ( $\text{CH}_3\text{OHCH}_3^+$ ), are generated when dimethyl ether is applied as a chemical ionization (CI) reagent gas.<sup>1</sup> According to Colorado and Brodbelt,<sup>3</sup> when DME reacts with compounds possessing

electron-releasing substituents such as a hydroxyl, methoxyl or amino group,  $[\text{M} + 13]^+$  adduct ions are typically produced via methylene addition reactions of  $m/z$  45 followed by the loss of a molecule of  $\text{CH}_3\text{OH}$ , but compounds with electron-withdrawing substituents such as carbonyl groups could form  $[\text{M} + 15]^+$  adduct ions via methyl addition reaction followed by the loss of a molecule of formaldehyde.<sup>3</sup> All of these previous studies were undertaken using a traditional internal ionization ion trap. However, since Finnigan MAT will no longer produce the traditional internal ionization ion trap mass spectrometer (ITMS), it is important to test the CI method in the newest configuration with an external source benchtop ion trap mass spectrometer (GCQ).

The advantage of the external ion source GCQ over the traditional internal ITMS is that by using external ionization, the ionization is separated from the ion storage and analysis so that only ions are allowed to enter the ion trap itself, all neutral molecules being pulled away by vacuum. Hence spectral consistency is maintained. In addition, space charge effects are minimized, so the resolution and sensitivity of the ion trap can be improved. In contrast, the traditional internal ITMS allows all CI reagent molecules and analytes to ionize and react inside the trap, and residual neutrals inside the trap will have more time to react with the analyte ions. Hence space charge effects and self-chemical ionization

\* Correspondence to: H.-F. Wu, Department of Chemistry, Tamkang University, Tamsui, Taipei Hsien, 25137, Taiwan.

Contract/grant sponsor: National Science Council of the Republic of China; Contract/grant number: NSC 83-2113-M-032-009.

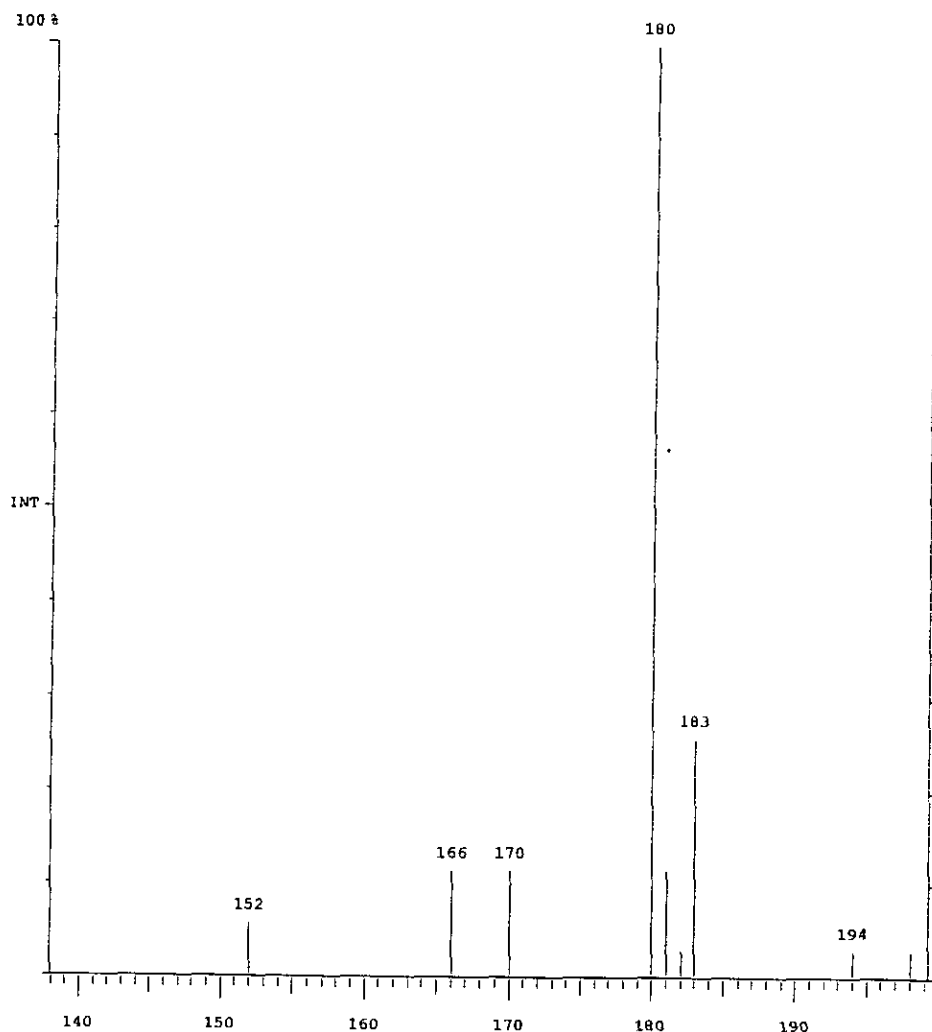


Figure 1. CAD mass spectrum of  $[\text{M} + 45]^+$  ions of dopamine.

**Table 1. CAD of low-abundance product ions of dopamine with dimethyl ether ions ( $m/z$  with relative abundances (%))**

[M + 15] <sup>+</sup> (168, 2%)	– NH <sub>3</sub> (151, 100%)
	– H <sub>2</sub> O (150, 3%)
	– C <sub>2</sub> H <sub>4</sub> (140, <1%)
	– CH <sub>2</sub> NH (139, 4%)
	– CH <sub>3</sub> NH <sub>2</sub> (137, 71%)
	– (CH <sub>3</sub> NH <sub>2</sub> + H <sub>2</sub> O) (119, 3%)
	– (CH <sub>3</sub> NH <sub>2</sub> + H <sub>2</sub> O + 28) (91, 2%)
[M + 45] <sup>+</sup> (198, 1%)	194, 2%
	– CH <sub>3</sub> (183, 26%)
	181, 10%
	– H <sub>2</sub> O (180, 100%)
	– C <sub>2</sub> H <sub>4</sub> (170, 11%)
	– CH <sub>3</sub> OH (166, 11%)
[M + 47] <sup>+</sup> (200, <1%)	– CH <sub>3</sub> OCH <sub>3</sub> (152, 3%)
	196, 20%
	195, 20%
	– CH <sub>3</sub> (185, 20%)
	– C <sub>2</sub> H <sub>4</sub> (172, 40%)
	171, 9%
	160, 10%
	– CH <sub>3</sub> OCH <sub>3</sub> (154, 100%)
	153, 10%

reactions can occur.<sup>4,5</sup> Owing to the huge amount of neutrals in the conventional ion trap (including DME or analytes), the primary ionization can lead to space charge effects, which have been a serious problem for the traditional ion trap. We consider it important to test the CI method in this new external ionization configuration of the ion trap. The reason why DME was chosen as the reagent gas in this study is that it is the most versatile CI reagent that has been applied in the traditional ion trap in the past.<sup>1,2</sup>

In our hands, the external ion trap mass spectrometer first demonstrated its excellent sensitivity in the MS/MS mode in a series studies of ion–molecule reactions of anthraquinones, tricyclic antidepressants, flavones and flavanones with dimethyl ether. Even for product ions with relative abundance as low as 0.01%, collision-activated dissociation (CAD) experiments were successfully performed. This is a very important feature for an analytical instrument because new types of experiments could be designed based on this aspect, such as differentiation of isomers or other pairs of compounds with only slight structural differences, for the detection of analytes with very low concentrations or for the investigation of product ions obtained at very low abundance in the full-scan spectra.

In this study, the detection limits for DME CIMS and for CAD of dopamine were determined using an external CI source quadrupole ion trap mass spectrometer. This work demonstrates the possibility of applying a commercial ion trap instrument to perform high-sensitivity measurements with low detection limits in the MS/MS mode. CAD experiments on ions with relative

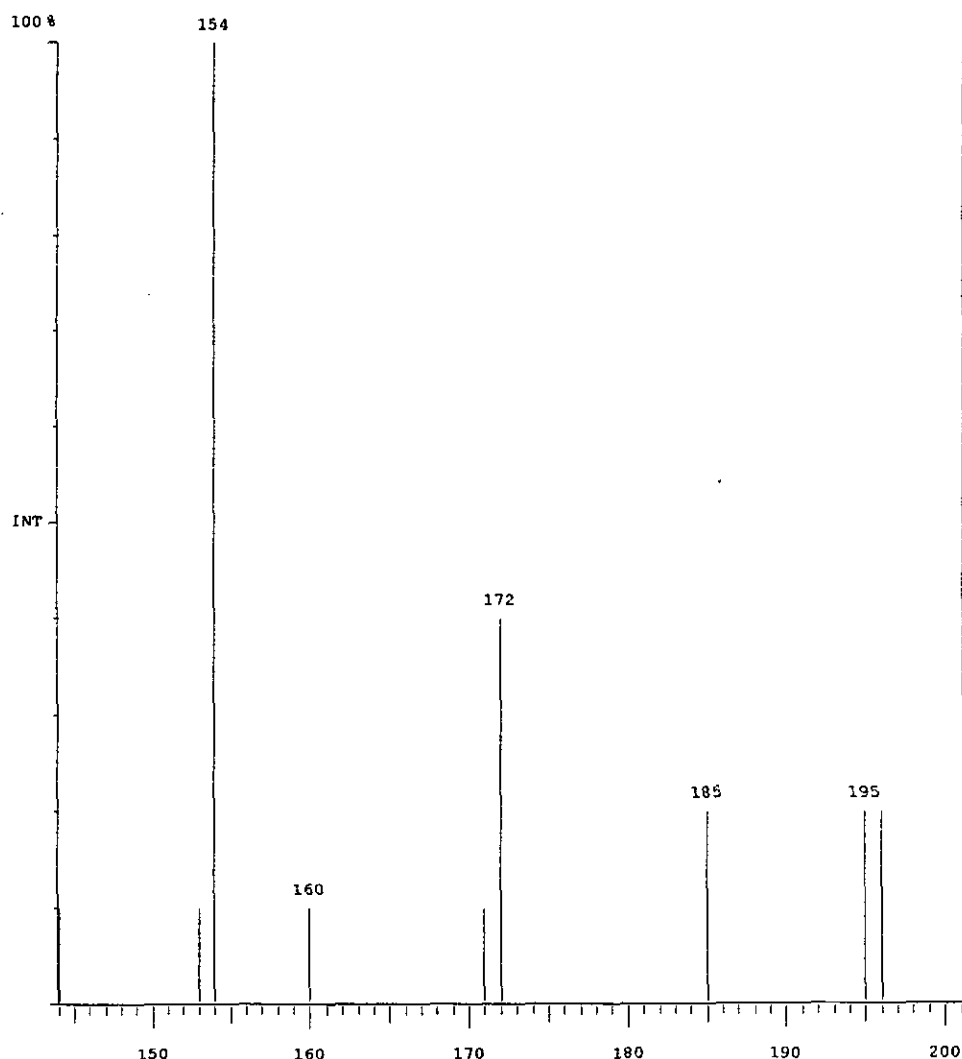


**Figure 2. CAD mass spectrum of [M + 47]<sup>+</sup> ions of dopamine.**

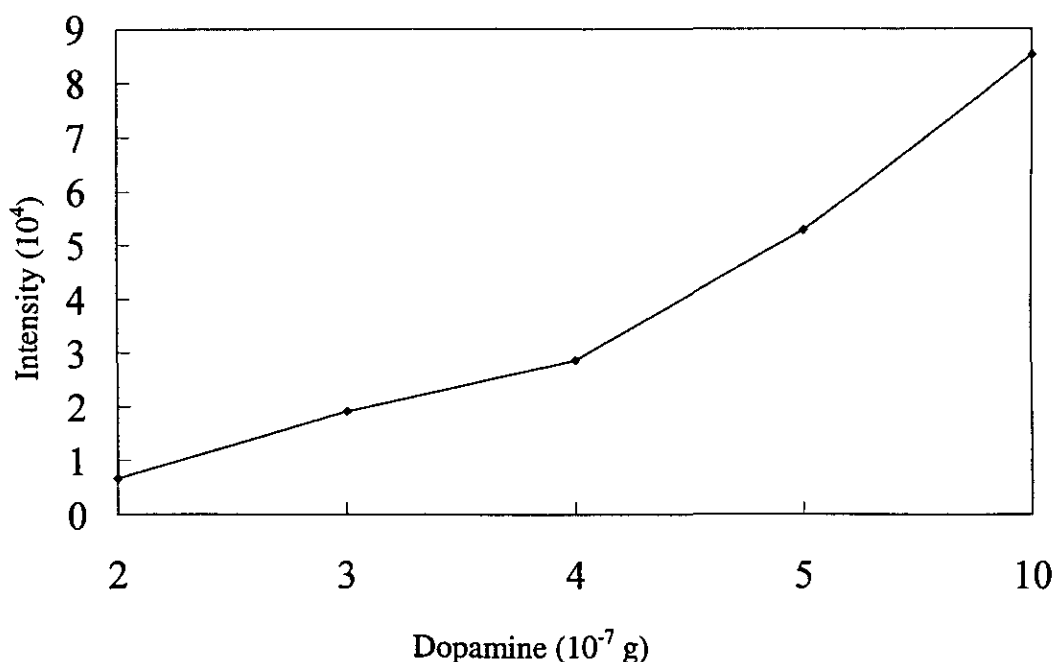


Figure 3. Calibration graph for the determination of detection limits.

abundance as low as 0.04–2.43%, formed as ion–molecule products of dopamine, have been successfully performed. Information about detection limits with the use of DME as the reagent gas in CI is provided.

All experiments were performed using a Finnigan MAT GCQ ion trap mass spectrometer, equipped with an external EI/CI source. DME was used as the CI reagent gas. The instrument was operated in the mass-selective instability mode. The relative abundance of  $m/z$  45 and 47 ions of DME was 3:1. The pressures of He buffer gas and DME were 1 and  $8 \times 10^{-5}$  mTorr, respectively (1 Torr = 133.3 Pa). The pressure in the ion source region was  $\sim 1$  mTorr and that in the ion trap mass analyzer was  $\sim 10^{-6}$  Torr. The temperature of the source region was maintained at 200°C unless stated otherwise. The ion injection time was 25 ms. Collisional experiments were performed by application of a supplementary tickle voltage to the end-caps of the ion trap at  $q_z = 0.225$ . The collisional activation time was 15 ms. The signal width for selection of the parent ions was 0.1–1 u; the collision energy for fragmentation of the parent ions was 0.7–1.0 V. Samples were introduced into the ion source region via a temperature-controlled direct insertion probe (DIP) to assist the desorption of the sample. The probe tip was heated to 250°C at a rate of 100°C min $^{-1}$ .

The DME ions were allowed to react with dopamine, introduced as neutrals from a temperature-controlled direct insertion probe to generate a series of ion–molecule reaction products including  $[M - H]^+$ ,  $[M + 13]^+$ ,  $[M + 15]^+$ ,  $[M + 45]^+$ ,  $[M + 47]^+$ ,  $M^{++}$  and  $[M + H]^+$  ions and fragment ions. Among these ions, most adduct ions have very low relative abundances, e.g.  $[M + 47]^+ < 1\%$ ,  $[M + 45]^+ = 1\%$  and  $[M + 15]^+ = 2\%$ . Most of time they could not be observed at all in the full-scan spectra, yet quantitative information can be obtained from GCQ, which means that they do exist. Moreover, since the GCQ instrument possesses the ability to perform MS/MS on low-abundance ions, these product ions still could be isolated and CAD experiments successfully undertaken. Table 1 gives the CAD results for  $[M + 47]^+$ ,  $[M + 45]^+$  and  $[M + 15]^+$  ions of dopamine, which were formed from the reactions of dopamine with DME ions. Figures 1 and 2 show the CAD spectra of  $[M + 45]^+$  and  $[M + 47]^+$  ions of dopamine, respectively.

In order to gain a better understanding of the CAD detection limit in the external source ion trap mass spectrometer, the following experiments were performed. A series of

standard solutions of dopamine were prepared in methanol at concentrations of  $1 \times 10^{-4}$ ,  $2 \times 10^{-4}$ ,  $3 \times 10^{-4}$ ,  $4 \times 10^{-4}$ ,  $5 \times 10^{-4}$  and  $1 \times 10^{-3}$  g ml $^{-1}$ . Volumes of 1  $\mu$ l of the standard solutions of dopamine were first subjected to an evaporation step by a heater to eliminate the solvent and then it was introduced to the ion source region of the GCQ via a temperature-controlled DIP. Limits of detection runs were confirmed by having a signal-to-noise ratio of 10. The absolute detection limit of CAD found in this study is  $8 \times 10^{-11}$  g for  $[M + 47]^+$  ions of dopamine; the absolute detection limit for the CI mass spectrum of GCQ by DIP is  $2 \times 10^{-7}$  g for dopamine. Figure 3 shows the calibration graph for determining the detection limits.

From this study, we conclude that the GCQ ion trap mass spectrometer possesses excellent tandem mass capability and gives low detection limits for CAD. This can lead to the understanding of the bonding properties of these low-abundance ion–molecule adduct ions. Further, with the external chemical ionization configuration, space charge effects and self-chemical reactions during ion–molecule reactions in the ion trap mass spectrometer, which was a problem with the traditional ion trap mass spectrometer, can be avoided. Hence the reproducibility, sensitivity and resolution in the GCQ ion trap are greatly enhanced.

The support of the National Science Council of the Republic of China (Grant No. NSC 88-2113-M-032-009) is gratefully acknowledged.

Yours,

HUI-FEN WU\* and YA-PING LIN

Department of Chemistry, Tamkang University, Tamsui, Taipei Hsien, 25137, Taiwan

#### References

1. Brodbelt JS, Liou C-C, Donovan T. *Anal. Chem.* 1991; **63**: 1205.
2. Brodbelt JS, Louris JN, Cooks RG. *Anal. Chem.* 1987; **59**: 1278.
3. Colorado A, Brodbelt J. *Anal. Chem.* 1994; **66**: 2330.
4. Eichelberger JW, Budde WL, Slivon LE. *Anal. Chem.* 1987; **59**: 2730.
5. McLuckey SA, Glish GL, Asano KG, Van Berkel GJ. *Anal. Chem.* 1988; **60**: 2312.